RESEARCH PAPER

Quantification in MALDI-MS imaging: what can we learn from MALDI-selected reaction monitoring and what can we expect for imaging?

Tiffany Porta · Antoine Lesur · Emmanuel Varesio ·
Gérard Hopfgartner

Abstract Quantification by mass spectrometry imaging (Q-MSI) is one of the hottest topics of the current discussions among the experts of the MS imaging community. If MSI is established as a powerful qualitative tool in drug and biomarker discovery, its reliability for absolute and accurate quantification (QUAN) is still controversial. Indeed, Q-MSI has to deal with several fundamental aspects that are difficult to control, and to account for absolute quantification. The first objective of this manuscript is to review the state-of-the-art of Q-MSI and the current strategies developed for absolute quantification by direct surface sampling from tissue sections. This includes comments on the quest for the perfect matrix-matched standards and signal normalization approaches. Furthermore, this work investigates quantification at a pixel level to determine how many pixels must be considered for accurate quantification by ultraviolet matrix-assisted laser desorption/ionization (MALDI), the most widely used technique for MSI. Particularly, this study focuses on the MALDI-selected reaction monitoring (SRM) in rastering mode, previously demonstrated as a quantitative and robust approach for small analyte and peptide-targeted analyses. The importance of designing experiments of good quality and the use of a labeled compound for signal normalization is emphasized to minimize the signal variability. This is exemplified by measuring the signal for cocaine and a tryptic peptide (i.e., obtained after digestion of a monoclonal antibody) upon different experimental conditions, such as sample stage velocity, laser power and frequency, or distance between two raster lines. Our findings show that accurate quantification cannot be performed on a single pixel but requires averaging of at least 4–5 pixels. The present work demonstrates that MALDI-SRM/MSI is quantitative with precision better than 10–15 %, which meets the requirements of most guidelines (i.e., in bioanalysis or toxicology) for quantification of drugs or peptides from tissue homogenates.

T. Porta · A. Lesur · E. Varesio · G. Hopfgartner (✉)
Life Sciences Mass Spectrometry, School of Pharmaceutical Sciences, University of Geneva, University of Lausanne, Quai Ernest-Ansermet 30, 1211 Geneva 4, Switzerland
e-mail: gerard.hopfgartner@unige.ch

Present Address:
T. Porta
FOM Institute AMOLF, Science Park 104, 1098 XG Amsterdam, The Netherlands

Present Address:
A. Lesur
Luxembourg Clinical Proteomics Center, Centre de Recherche Public de la Santé (CRP-Santé), 1A-B rue Thomas Edison, 1445 Strassen, Luxembourg

Introduction

Mass spectrometry imaging (MSI) is nowadays established as a powerful approach for the direct screening and mapping of molecular species in complex biological samples such as tissues. MSI has opened new perspectives in drug discovery and development and biomarker discovery by correlating identification and spatial localization of the compounds of interest within the biological matrix, down to the cellular level [1–3]. One of the strengths of MS-based techniques for low molecular weight compounds analysis, including MSI, is the ability to distinguish between drugs and their metabolites and

T. Porta et al.

other endogenous molecules, such as lipids, as long as the mass resolving power or tandem MS experiments provide sufficient selectivity. As MSI is mostly employed to show the analyte spatial distribution in samples, the ultimate goal would be adding, in a single experiment, the accurate quantification of the targeted analytes. For most applications, the reproducibility is of prime importance, and any efforts must be deployed in the method development to achieve robust and accurate comparison between samples (e.g., tumor or healthy tissue) by using normalization of results [4].

Several developments have been made to address these challenges [5, 6]. However, accurate/absolute quantification from tissue sections by ultraviolet matrix-assisted laser desorption/ionization (MALDI), the most commonly used technique for MSI, still requires additional research efforts to establish the best practices. Currently, MALDI-MSI is used for analyte spatial distribution visualization, while quantitative whole-body autoradiography (QWBA) remains to be the gold standard method in drug discovery and development for absolute quantitation, as long as radiolabeled drugs are available [7]. After organ dissection and homogenization, capillary electrophoresis [8] or liquid chromatography [9, 10] combined with mass spectrometric detection was also used to cross-validate MSI results showing the potential of the technique. Furthermore, there is a recurrent need to establish protocols to evaluate the quantitative potential of MSI, including precision, accuracy, and repeatability. MSI relies on the direct analysis of thin (e.g., 5–20 μm) tissue sections, without any chromatographic separation after surface sampling and prior to mass spectrometric detection. Therefore, selectivity is important to avoid interfering ions from the MALDI matrix or from endogenous compounds present in the biological tissue.

Quantitative MSI (Q-MSI) on tissue sections has to deal with several fundamental aspects such as analyte recovery from the tissue and ionization matrix effects. An analyte present in a tissue may have different non-covalent or covalent interactions with the tissue, which results in different recoveries. In addition, the overall sensitivity of the method is strongly analyte dependent in part due to the absence of chromatographic separation, which enhances the effect of ionization competition and variation in ionization efficiencies between compounds [11]. In particular, endogenous species, such as highly abundant phospholipids in cell membranes, affect the analyte's signal intensities. The use of internal standards and specific preparation of calibration standards is therefore critical. As illustrated in Fig. 1, none of the common strategies (i.e. in-solution, on-tissue, and in-tissue) can cope with all of these limitations (matrix effects, extraction efficiency, sample preparation) even when using labeled internal standards [12].

The in-solution approach for building a calibration range consists of spotting standards onto the target plate aside the tissue section. This approach does not compensate for tissue
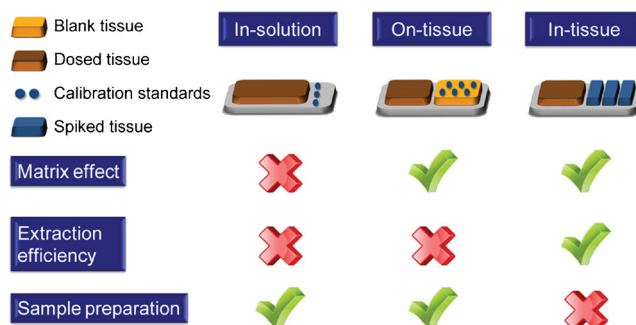
Fig. 1 Strategies developed for Q-MSI and their respective main advantages and drawbacks. The *in-solution* and *on-tissue* strategies make use of calibration range deposited onto the sample target plate or onto a blank tissue section, respectively. The *in-tissue* strategy relies on dosed surrogate tissue that mimics the analyte's behavior in its biological environment. Only the *in-tissue* strategy accounts for both matrix effect and extraction efficiency, but it relies on a complex and time-consuming sample preparation, unlike the *in-solution* and *on-tissue* strategies. Adapted and completed from Hamm et al. [12]

ionization effects or for inhomogeneous analyte extraction efficiency.

The *on-tissue* strategy, where the standards are spotted onto a blank tissue, allows taking into account ionization effects. As an example, Nilsson et al. demonstrated that compounds administered by inhaled delivery at standard pharmacological dosage can be quantitatively detected by MALDI-MSI, using both MS and MS/MS modes, with acceptable accuracies and precisions [13]. Another study correlated the MALDI-MSI response with quantitative LC-MS/MS performed on adjacent tissue sections and, after harvesting from rats, several single doses of olanzapine at different concentrations [14]. Goodwin et al. also employed MALDI-MSI to map commonly employed PET ligands in rat brain tissue sections [15]. However, the on-tissue approach does not account for droplet dispersion on the tissue and does not reflect the actual analyte concentration per gram of tissue (i.e., signal recorded expressed versus amount [in mol or g] spotted).

Finally, the *in-tissue* strategy, referred as "matrix-matched standard" and based on dosed surrogate tissue, has been widely described for the quantification of trace metals in tissue sections by LA-ICP-MS [16]. Recently, Groseclose et al. developed a surrogate tissue model for drug quantification by MALDI-MSI [17]. The protocol relies on tissue homogenates spiked with a range of increasing drug concentrations across 3 orders of magnitude with good linearity and adequate inter-section homogeneity with a signal variation of 16 %. Both *on-tissue* and *in-tissue* approaches are particularly adapted to single-organ drug distribution studies. The *in-tissue* strategy is best suited to account for both analyte extraction and ionization effects. Quantitative results were directly expressed in amount of analyte per mass of tissue. With multiple-organ or whole-body tissue section analysis, the procedure becomes time-consuming and relies on a large amount of nontreated tissue material [12]. In addition, cells might be disrupted

during the homogenization process and the material extracted from these sections may not accurately represent the actual situation from the intact tissue sectioned.

To address MS ionization suppression or enhancement effects dependent of the tissue type, different strategies were described. Stoeckli et al. suggested to determine a quantification factor named tissue-specific ionization effect (TSE). TSE factors are measured for different tissues by spraying a standard solution of the analytes onto blank tissue sections [18]. TSE factors were then used to calculate the neat drug levels in the different tissues. This label-free approach is particularly suitable in early drug discovery where no labeled version of the drug is available. However, this strategy only enables relative quantification and assumes that analyte extraction within a tissue remains constant. A variant of this method proposed to use a "tissue extinction coefficient (TEC)" as a normalization factor [12]. The TEC approach relies on (i) the determination of tissue- and drug-specific TEC after spraying the analyte standard solution (i.e., comparison between the signals from the analyte measured "on tissue" versus "on plate"), independent of the analyte's concentration [12], and (ii) an analyte calibration series spotted near the dosed tissue section. A calibration curve is subsequently built integrating TEC and mean intensity values of the analyte signals. This allows to determine the amount of drug per gram of tissue surface unit. Although this approach does not take into account the extraction efficiency specific to each compound, results were consistent with other analytical techniques such as liquid chromatography mass spectrometry [19]. The strategy has been successfully applied to the absolute quantification of several drugs in dosed mice and also for endogenous compounds, either by MALDI-MSI or LESA-MS [5, 12].

To account for the inherent signal variability, normalization of the signal is mandatory to allow for intra- and/or inter-comparison between tissues/samples. Several papers report the normalization of all spectra against the total ion current (TIC) and prove its suitability to reduce the influence of inhomogeneous matrix coating, that is critical in MALDI-MS imaging experiments [14, 15, 19, 20]. However, if one background ion (interference) dominates in one of the groups, the TIC normalization can lead to incorrect results [21]. In this case, a more robust approach such as normalization with the median intensity of the peaks may be considered because it is less prone to outliers [22].

Källback et al. recently developed an MSI software for the quantification of drugs and neuropeptides in tissue sections [23]. Among the different normalization methods, the use of labeled internal standards (ISTDs) showed the best linear regression fit [24, 25]. ISTD can be a labeled version of the analyte [26–28, 23], a structural analogue [29], or an endogenous signal (e.g., a peptide in the same mass range as the targeted analyte [30] or a lipid species [31]). In Q-MSI, ISTD normalization compensates for signal variations resulting in

difference in analyte extraction, co-crystallization, and ionization [32], assuming that the ISTD is homogenously distributed over the region of interest. In targeted approach, the use of isotopically labeled ISTD is proven relevant for the quantification of both endogenous [33] and exogenous compounds [26, 34] (see Electronic Supplementary Material (ESM) Table S1). Ellis et al. stated that "Q-MSI requires the use of internal standards for calibration of analyte signal, an applied method is only suitable for a specific analyte/sample combination […] Q-MSI necessitates a targeted analysis where only one or several molecules can be analyzed" [35].

The present investigation focuses on the source and MS experimental parameters that influence the sensitivity and the accuracy of the signal measured when combining selected reaction monitoring (SRM) and rastering modes on a MALDI-triple quadrupole mass analyzer. This platform has been previously successfully used for quantifying pharmaceuticals [36, 37] or peptides [38] in biological matrices. The sample stage velocity, the laser frequency, the distance between two raster lines, and the MS duty cycle will be evaluated for Q-MSI performed in raster MALDI-SRM/MSI. This is exemplified by characterizing the variability of the signal measured for cocaine and a tryptic peptide obtained after digestion of a monoclonal antibody. The instrumental variability is compound independent, and our concept may be adapted to a range of compound classes, such as lipids.

Experimental details

Chemicals and reagents

Cocaine (COC) and cocaine-d_3 (COC-d_3) were provided by Lipomed (Arlesheim, Switzerland). Methanol (MeOH, HPLC grade) and acetonitrile (ACN) were provided by Sigma-Aldrich (Buchs, Switzerland). α-Cyano-4-hydroxycinnamic acid (CHCA) was provided by Fluka (Buchs, Switzerland). Formic acid (HCOOH) was purchased from Merck (Darmstadt, Switzerland). Water was purified with a Milli-Q Gradient A10 system (Millipore, Bedford, MA, USA). Solutions of recombinant human monoclonal antibody (MM: 145.157 kDa, concentration: 53.8 μg/μL) and its isotope version labeled on threonines ($^{13}C4$, $^{15}N1$, Δm 5 u– 5.54 μg/μL), used as an internal standard (IS), were obtained from Novartis Pharma AG (Basel, Switzerland).

Preparation of drug standards and matrix solutions

The widespread dried droplet method was used to prepare MALDI samples. A standard solution containing both COC and COC-d_3 was prepared at a concentration of 2 pg/μL (unless otherwise stated) in ACN:H$_2$O:HCOOH (60:40:0.1, $v/v/v$) from individual stock solutions of 1 mg/mL in MeOH.

The mixture was then mixed 1:1 (*v/v*) with CHCA matrix solution 10 mg/mL in ACN:H$_2$O:HCOOH (60:40:0.1, *v/v/v*). Sample spots were prepared by loading 1 μL of the cocaine/CHCA solution on the stainless steel MALDI plate, so that the final amount of standards was of 1 pg in each MALDI spot. Four MALDI spots were analyzed per experimental condition (i.e., four replicates per condition).

Tryptic digestion

Tryptic digestion, 4-sulfophenyl isothiocyanate (SPITC) derivatization, and purification by SPE of a monoclonal antibody and its stable isotope-labeled version were performed in a similar way as described in reference [39]. The digests were directly eluted in a CHCA matrix solution (10 μg/μL, in 60/40 ACN/TFA aq. 0.1 %). One microliter was spotted onto the MALDI target according to the dried droplet method in four replicates. The estimated amount of mAb in a single spot is 94.4 ng/spot (internal standard 43.7 ng/spot).

MALDI mass spectrometry imaging

Acquisitions were performed on a MALDI-triple quadrupole linear ion trap mass spectrometer (AB Sciex, Concord, ON, Canada) equipped with a 355-nm frequency-tripled Nd:YAG laser (elliptic beam shape of 100 by 200 μm, in the *x*- and *y*-dimensions, respectively). Data were acquired in the positive ion ionization mode using the selected reaction monitoring mode. The SRM transitions monitored were m/z 304>m/z 182 for cocaine [declustering potential (DP)=70 V; collision energy (CE)=27 eV] and m/z 307>m/z 185 for cocaine-d$_3$ (DP= 70 V; CE=27 eV). General operating conditions were as follow: data acquisition mode=horizontal rastering mode (following the *X*-dimension), repetition rate laser=50–1000 Hz; MALDI source and q0 region pressures of 1 Torr and 8 mTorr, respectively; vacuum gauge in q2=2.4×10^{-5} Torr (nitrogen was used as collision gas); entrance potential=10 V; and quadrupole resolution that was set to unit. Unless otherwise stated, laser energy was kept constant at 50 μJ and calibrated prior the analysis using a power/energy meter (EPM1000; Coherent, Portland, OR, USA) equipped with a pyroelectric energy sensor (J25LP-3A; Coherent, Portland, OR, USA). The distance between two line scans (pitch), the dwell time (DT) set for each transition, the plate stage velocity, and the resulting pixel sizes are given in Table 1. The signals were recorded at each position of the samples, and 2D maps based on each SRM transition were generated. In our experimental setup, the minimum step achievable in between two raster lines with the motors positioning the sample stage was of 30 μm.

The MALDI-SRM/MS imaging of the peptide spots was performed using the rastering mode with a pitch of 100 μm. The SRM transitions m/z 1533.6>m/z 732.3 for the native peptide AEDTAVYYCAR and m/z 1538.6>m/z 732.3 for the isotope-labeled peptide were recorded. For the analysis of peptides, the operating conditions were: laser repetition rate=1 kHz, MS total scan time=120 ms, and laser shots per pixel=120.

Software for data acquisition and processing

M3Q Server software based on a LabView platform (AB Sciex) controlled the MALDI source and its laser. Analyst 1.5 software (AB Sciex) was used for mass spectrometer control and for data collection. PeakView software (v.1.0.0.3, AB Sciex) was used for raw data processing (.wiff files). A dedicated script was provided by Eva Duchoslav (AB Sciex) to convert raw MS data files (.wiff format) into an .img file format that is compatible with the TissueView software (v.1.0, AB Sciex), used for SRM/MS image generation and processing. TissueView software offers several mathematical functions available for processing MS imaging. To generate the so-called "normalized images" for cocaine, the function "divide" in the "tools" menu was used. In the case of MS image (.img file) acquired in the SRM mode, an .img file is created for each SRM transition. The divide function consists in a normalization of one image (i.e., based on the SRM trace for cocaine) by another one on a "pixel-by-pixel" basis. The region(s) of interest (ROI) is(are) then drawn manually in TissueView on this new image processed by the software; the data extracted are then imported in Excel for further statistical calculations. The same surface was used for the four spots acquired under the same conditions. All images are displayed in the "voxel" mode in the TissueView software.

Results and discussion

Definition of spatial resolution, pixel, and oversampling

The spatial resolution is one of the key parameters that significantly impacts the molecular information, the sensitivity, and the analysis time [3]. Nonetheless, improving the spatial resolution (i.e., by the acquisition of smaller pixels) leads to a significant decrease of sample throughput and sensitivity and also increases the amount of data generated. For these reasons, the experimental parameters strongly affect the generation of MS images. A *pixel* is the smallest measurable unit of a raster image, defined by its (*X,Y*)-coordinates. A voxel is defined as a volume element, i.e., the 3D analogue of a 2D pixel. In MSI, a voxel is defined by its coordinates in the raster image and by its intensity (i.e., given by the MS signal recorded). Several instrumental parameters may affect the size of pixel (i.e., in its *X*- and *Y*-dimensions), as depicted in Fig. 2. It begins with the laser beam diameter and the mode of acquiring the MS

Table 1 Description of the experiments related to the analysis of MALDI spots containing COC and its deuterated analogue COC-d_3. Two SRM transitions were monitored in each experiment

Set ID	Varying parameter	Stage velocity mm/s	Laser Frequency (Hz)	Nb shots/pixel[a]	SRM method DT (ms)	TST (ms)	Pixel size (acquired) X (μm)	Y (μm)
Set I	Y-step	1	1000	5	20	50	50	30[b]
		1	1000	5	20	50	50	50[b]
		1	1000	5	20	50	50	100
		1	1000	5	20	50	50	200
Set II	Plate speed	1	1000	20	20	50	50	100
		2	1000	20	20	50	100	100
		3	1000	20	20	50	150	100
		4	1000	20	20	50	200	100
Set III[c]	Frequency (same MS method)	1	50	2.25	45	100	100	100
		1	100	4.5	45	100	100	100
		1	200	9	45	100	100	100
		1	500	22.4	45	100	100	100
		1	1000	45	45	100	100	100
Set IV[c]	Frequency (same number of shots per pixel)	1	50	5	100	210	210	100
		1	100	5	50	110	110	100
		1	200	5	25	60	60	100
		1	500	5	10	30	30	100
		1	1000	5	5	20	20	100
Set V	Laser shots per pixel	1	1000	5	5	20	20	100
		1	1000	10	10	30	30	100
		1	1000	20	20	50	50	100
		1	1000	45	45	100	100	100
		1	1000	95	95	200	200	100
Set VI	Acquisition of square pixels	1	1000	20	20	50	50	50[b]
		2	1000	20	20	50	100	100
		4	1000	20	20	50	200	200

[a] The number of laser shots per pixel is calculated as a function of the laser frequency (i.e., number of laser shots per second) and the dwell time (DT) set for each SRM transition as follows: Laser shots per pixel=Frequency (Hz)×DT (s)

[b] Images acquired using the oversampling method

[c] Both experimental sets III and IV are used to assess the influence of the laser frequency on data quality: (i) Set III uses the same SRM method in all conditions, which changes the number of laser shots per pixel, and (ii) set IV relies on different SRM methods adjusted to maintain the number of laser shots per pixel to 5, with constant sample stage velocity and varying laser frequency
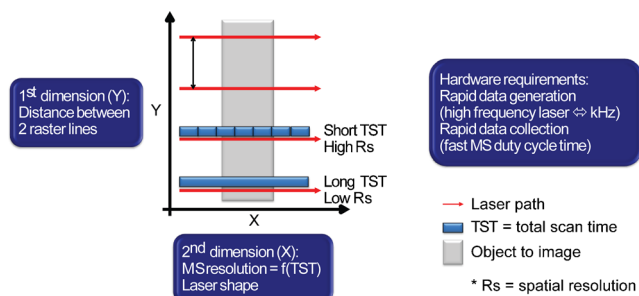
Fig. 2 Definition of the pixel and factors influencing the spatial resolution and the analysis time in microprobe MS imaging performed in continuous laser raster sampling

images, namely discrete or rastering. When the image is acquired in the discrete mode, the pixel size is defined by the pitch set between two adjacent ablation spots. Spot-by-spot analysis may result in several hours of acquisition time. To increase the throughput in microprobe MALDI-MSI approaches, acquisitions are performed in a continuous raster sampling mode [40, 41] where the sample stage moves laterally at constant velocity and the laser operates at a fixed repetition rate. Combining a high sample stage velocity (e.g., 4 mm/s) with a high-frequency laser (in the range of kHz) requires rapid data collection obtained by MS instruments with short cycle time such as time of flight (TOF) or triple quadrupole (QqQ) operated in the SRM mode.

In the rastering mode, the lateral spatial resolution (X-dimension) becomes a function of the sample stage velocity and the MS cycle time of the experiment, also referred as total scan time (TST). The lateral spatial resolution (R_s) is calculated according to Eq. 1

$$\text{Lateral } R_s = \text{Plate stage velocity} \times \text{TST} \qquad (1)$$

In SRM experiments, the TST is defined as follows:

$$\text{Total scan time (s)} = n(\text{DT} + \text{PT}) \qquad (2)$$

where n is the number of transition(s) monitored, DT is the dwell time set for each transition, and PT is the pause time between each transition (i.e., 5 ms in our instrument).

If the TST is long, the resulting pixel size in the X-dimension will be larger and limited spatial information is obtained (Fig. 2), while on the opposite, if the TST is short, smaller pixels can be acquired resulting in a significant improvement in the lateral resolution and spatial information provided.

In the vertical dimension (Y-axis), the spatial resolution is defined by the distance between two laser line scans with the constraints of the laser beam dimensions and the sample stage motor pitch. To generate an image with pixel size smaller than the beam of the laser, the oversampling method is applied, where the raster increment of the sample stage movement is smaller than the laser beam dimensions [42, 43, 41]. The laser used in this study has an elliptic shape of 100×200 μm in the x- and y-dimension, respectively. The first set of experiments (set I, Table 1) showed an intra-spot variation comprised between 20 and 35 % (inter-spot variability <15 %) for COC and its deuterated analogue COC-d_3, independently from the Y-step used (ESM Table S2). This suggests the absence of influence of Y-step, i.e., oversampling, in the signal variability. Although the absolute signal for both COC and COC-d_3 increases with the pixel size (i.e., more material ablated), the COC/COC-d_3 ratio remains constant (ESM Fig. S1). Resulting MS images are displayed in Fig. 3. The inter-spot variability gives better results for both raw and normalized data (ESM Table S2). The precision of the sample stage positioning plays also a role in the definition of the spatial R_s in the Y-dimension. In our instrumental setup, the minimum incremental step allowed by the motor in this direction is of 30 μm.

Laser energy

The laser energy is an important parameter in the desorption/ablation process of molecules and ions in MALDI and depends on the source geometry and instrument type [44, 45]. With the MALDI-QqQ$_{\text{LIT}}$ instrument used in the present study, Corr et al. reported that higher laser fluence provides better signal, but on cost of carryover [46]. With higher laser energy, an increase of the absolute signal for COC is measured; however, the quality of the MS images is decreased. A spread of the matrix is observed with laser energy above 60 μJ (i.e., "snowplow effect"; ESM Fig. S2), resulting in the delocalization the analytes from their original position within the spot.

Sample stage velocity

When varying the sample stage velocity (ESM Table S3, set II), it has been observed that higher velocities result in higher signal intensities but also show higher intra-spot variability within a single population that is not reduced after pixel-by-pixel normalization. Interestingly, the inter-spot variability is not affected by the sample stage velocity and is lower than 20 % even at high velocity (e.g., 4 mm/s), which is favorable to high-throughput analysis. At lower sample stage velocities, lower signal may be explained by ionization suppression due to higher ions density during desorption, as previously reported by Spraggins and Caprioli [41].

Frequency and number of laser shots per pixel

As shown in Fig. 4(a–e), the number of laser shots per pixel influences the overall quality of the MSI results, since the signal intensity for COC is increasing when the laser frequency varies from 50 to 1000 Hz that correlates with previous findings [47]. Indeed, high repetition rate lasers (kHz range) allow, in a short amount of time, to perform signal averaging over a large number of measurements that increases sensitivity (i.e., increased signal/noise ratio) and reproducibility. This is also shown in Fig. 4(k) where the mean intra-spot variability significantly decreases from 71 % (50 Hz) to 18 % (1000 Hz). However, the pixel-by-pixel normalization with a labeled reference compound does not compensate for intra-spot variability at lower laser repetition rate, but this variability remains constant from spot to spot (inter-spot variability, ESM Table S4).

As a matter of fact in rastering mode, when increasing the laser frequency and keeping the number of shots per pixel constant, the total scan time is reduced as well as the pixel size (set IV, Table 1). This is beneficial for the MS image resolution because the number of pixels increases per surface area (Fig. 4(f–j)). Nevertheless, due to the low number of shots per pixel, the intra-spot variation fluctuates between 33 and 50 %, which is detrimental for accurate quantification (Fig. 4(l), ESM Table S5). Similar observations are made when the laser

**Fig. 3** (**a**) Optical images of MALDI spots before (first upper spot of the column) and after the laser passed through the spots with 30, 50, 100, and 200-μm incremental steps of the sample stage (experimental set I). (**b**) MALDI-SRM/MS images based on the SRM trace (absolute area) of COC (1 pg spotted). Each MALDI-SRM-based image is given with its own scale intensity. The maximum intensities are arbitrary units given by TissueView software, 2900 for the pixels of 50×30 μm, 3500 for the pixels of 50×50 μm, 7050 for the pixels of 50×100 μm, and 9020 for the pixels of 50× 200 μm. The minimum intensity was set to 300 for all MS images. Pixel-to-pixel variability in one raster line from images acquired and generated with pixel size of (**c**) 50×50 μm (oversampling; variation of 26 % along the line) and (**d**) 50×200 μm (variation of 19 % along the line)
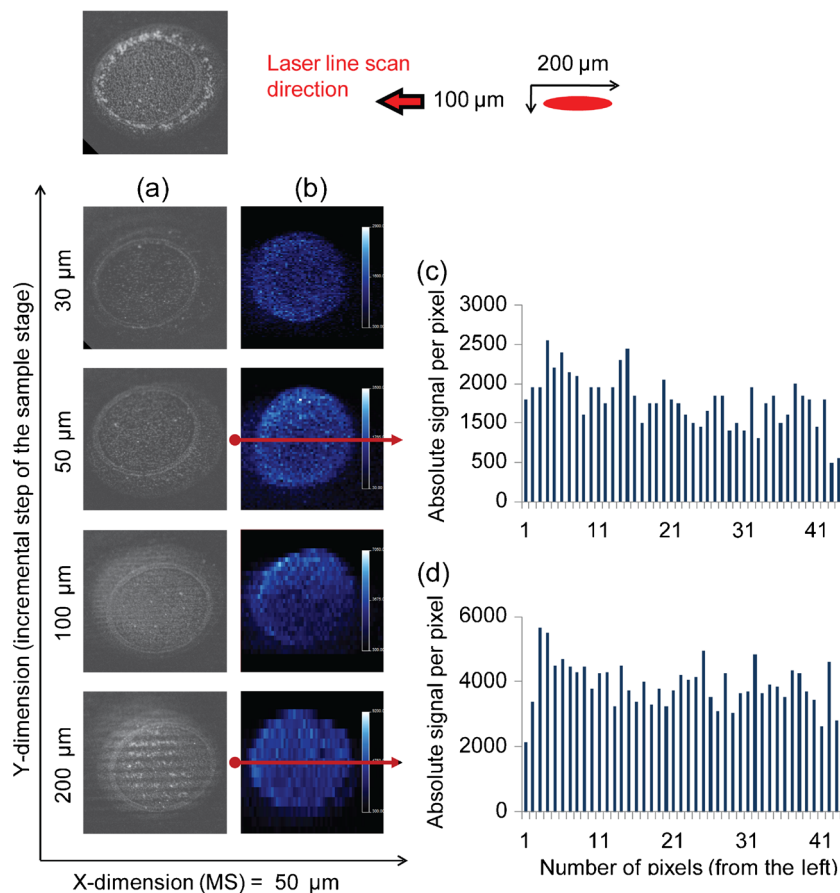
Fig. 4 MALDI-SRM/MS images of COC acquired at different laser frequency and MS conditions. Frequency (*I*max maximum intensity, a.u.): (**a**, **f**) 50 Hz (200), (**b**, **g**) 100 Hz (1000), (**c**, **h**) 200 Hz (1500), (**d**, **i**) 500 Hz (2000), and (**e**, **j**) 1000 Hz (4000). MS conditions for (**a**–**e**) experimental set III with fixed dwell times and cycle times and for (**f**–**j**) experimental set IV with variable dwell times and cycle times from slowest to fastest (see Table 1 for details). The graphs show the mean intra-spot variability (relative standard deviation (RSD) calculated for four different MALDI spots) in function of the laser frequency with (**k**) a varying number of laser shots per pixel (same MS acquisition parameters, set III) and (**l**) a constant number of laser shots (i.e., five shots) per pixel (varying MS acquisition parameters, set IV)
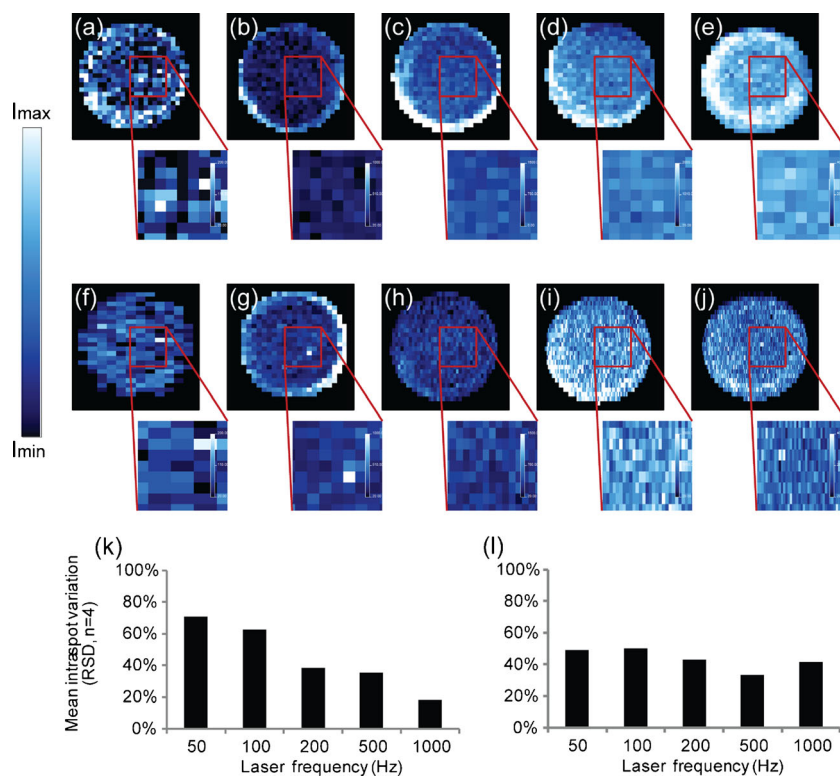
Fig. 5 Relative standard deviation as a function of the number of pixels averaged after acquisition of images with pixels of 50×50, 100×100, and 200× 200 μm and after processing of the high-resolution 50×50 μm *acquired* image into 100×100 and 200×200 μm *processed* images (see text and ESM Fig. S7 for details). Data based on (**a**–**c**) absolute COC signal and (**d**–**f**) COC/COC-d$_3$ ratio
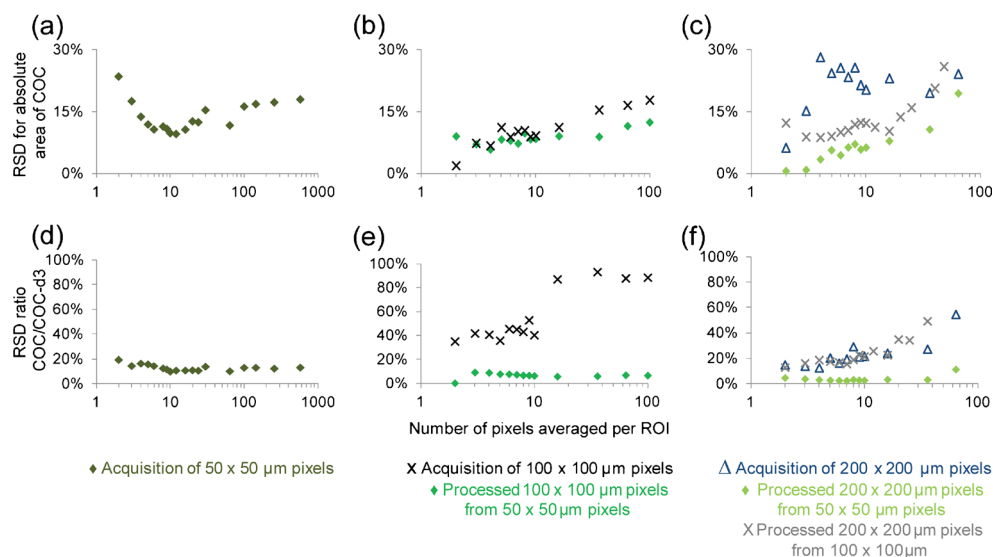
frequency is maintained at 1000 Hz and the dwell time is varied from 5 to 95 ms to increase the number of laser shots per pixel. The intra-spot variability is reduced by a factor of 2–3 with the highest number of laser shots per pixel (set V, ESM Table S6).

In summary, a precision better than 15 % can be obtained with 1 kHz laser. These findings correlate well with those of other studies where it is shown that high repetition rate lasers provide a much larger sample throughput compared to lower frequency lasers (i.e., 20–200 Hz) and increase the data quality [47, 48, 46].

Image processing and minimum number of pixels required for quantification

Norris et al. pointed out that a single mass spectrum (i.e., a single data point giving a pixel in the image) cannot be interpreted itself as a whole but has to be considered with the other elements [49]. Pixel-to-pixel comparison becomes tricky, and careful interpretation has to be done. In most of the cases presented above, results show high pixel-to-pixel variation within a single MALDI spot. Averaging four MALDI spots improves the reproducibility, and inter-spot variability is below 10 % in the best cases (ESM Tables S2, S3, S4, S5, and S6). This confirms that with MALDI-MSI, good spatial resolution affects adversely quantification variability.

To address the question of how many pixels should be considered at least for quantification, two different sets of images are compared: (i) images "A" corresponding to "low-resolution" images *acquired* relatively fast with large pixels (i.e., 100×100 or 200×200 μm) and (ii) images "B" that are *processed* from "high-resolution" images (i.e., pixels of 50×50 μm) and correspond to low-resolution images with pixels of 100×100 or 200×200 μm, respectively (for processing details, refer to ESM Figs. S7, S8, and S9 show the

resulting images before and after normalization, respectively). In general, high-resolution images (i.e., pixels of 50×50 μm) at low sample stage velocity results in less variation (Fig. 5(a)) considering that a minimum of 4 pixels have to be averaged to achieve a variation below 15 % (without normalization). Interestingly, the absolute signal for both COC and COC-d$_3$ remains in the same order whatever the condition in this experimental set VI (ESM Fig. S10a), but the overall variability is lower with acquisition of pixels of 50×50 μm in comparison with those acquired at lower resolution, i.e., namely 150×150 μm, 100×100 μm, and 200×200 μm (ESM Fig. S10b).

The normalization by a labeled reference compound does not compensate for intra-variability when large pixels are acquired but is still acceptable with the acquisition of 200×200 μm (relative standard deviation (RSD) ~15 %) and an average of 3 pixels (Fig. 5(f)). When processing image by averaging the signal over 4 or 16 pixels (to generate pixels of 100×100 or 200× 200 μm, respectively), the variation between 2 pixels of 100×100 or 200 μm×200 μm is already below a RSD of 10 %. Therefore, averaging signals over 4–5 pixels instead of comparing the pixel-by-pixel signals appear to be more suitable for quantitative analysis when less than 10 % of signal variability is required. However, the image resolution obtained with fast acquisition speed implying larger pixel sizes is still acceptable for higher MS image acquisition throughput (Fig. 5(f)).

Peptide quantification

Similar investigations have been performed on the tryptic digest of a monoclonal antibody and its stable isotope-labeled version used for normalization. Two ways of

normalization are evaluated for seven ROIs of different size (Fig. 6(a)):

1. The first approach consists in normalizing the intensity of the peptide recorded in the SRM mode by its labeled analogue on a pixel-by-pixel basis;
2. The second normalization technique is close to the method employed in bioanalysis or quantitative proteomics, which relies on the ratio between the chromatographic peak area or "pseudo peak" in the case of MALDI-SRM/MS operated in rastering mode. Here the signal of pixels from a defined area is averaged and normalized by the averaged signal of the IS from the same area.

Figure 6(b) shows MS images obtained for the native peptide and its labeled version as well as the pixel-by-pixel signal ratio (theoretical ratio of 2). At first glance, both normalization methods present very similar trends (Fig. 6(c, d)). This indicates that an MSI approach can provide the same performance in terms of accuracy and precision as standard quantification data processing that provided the number of pixels selected for quantification are sufficient. In this case, 10 pixels have to be considered to reach a reproducible area ratio with relative standard deviation below 10 % (Fig. 6(e)). This minimum of 10 pixels can probably be explained by the mode of crystallization in dried droplet that leads to a quasi-uniform distribution of small CHCA crystals. The ROI needs to cover at least enough crystals for good signal statistic, which calls for a more uniform matrix deposition techniques. It is noteworthy that the sample preparation plays a major role in the quality of the MS images generated, particularly the deposition of a thin,

microcrystalline matrix layer that covers homogenously the surface of the tissue section providing better spatial information with limited analyte delocalization [50, 51].

Conclusion

The present work makes use of a widespread dried droplet method to investigate various experimental parameters and, in particular, the pixel size for quantification in MALDI-SRM/MS imaging, with precision better that 10–15 %, comparable to those obtained with LC-ESI-MS/MS. The results highlight the limited impact of the sample stage velocity on the signal variability in a continuous laser raster sampling mode. However, a high laser frequency (i.e., 1 kHz) produces higher-quality data with minimum spot-to-spot variability and increased overall signal intensity. The laser energy should be carefully set to avoid snowplow effects which may hamper image resolution and quantification. While the analyte visualization can be realized at a single pixel level, accurate quantification needs an average of 4–5 pixels to compensate for instrumental variability and potential pixel-to-pixel matrix heterogeneity. Faster acquisition resulting in larger pixels shows more variability than slower acquisition combined with higher resolution (i.e., smaller pixels) but is more favorable for higher throughput. Finally, this work reinforces the fact that normalization with a reference compound, preferably a labeled version of the targeted analyte, is essential to reduce the signal variability and therefore increase data quality. The finding of the present study certainly remains valid for other types of mass analyzers such as TOF-TOF or QqTOF performing quantification in HR-SRM mode.

Fig. 6 Normalization method for peptide quantification. (**a**) Size of the region of interest (*ROI*), (**b**) MALDI-SRM/MS images for the peptide AEDTAVVYCAR obtained after digestion and derivatization of a monoclonal antibody, its stable isotope-labeled analogue (IS), and after pixel-by-pixel signal ratio (theoretical ratio of 2). Variation of the ratio peptide/IS after (**c**) pixel-by-pixel normalization and (**d**) area-by-area normalization as a function of the number of pixels considered per ROI. (**e**) Inter-spot variability (RSD%) in function of the number of pixels selected per ROI
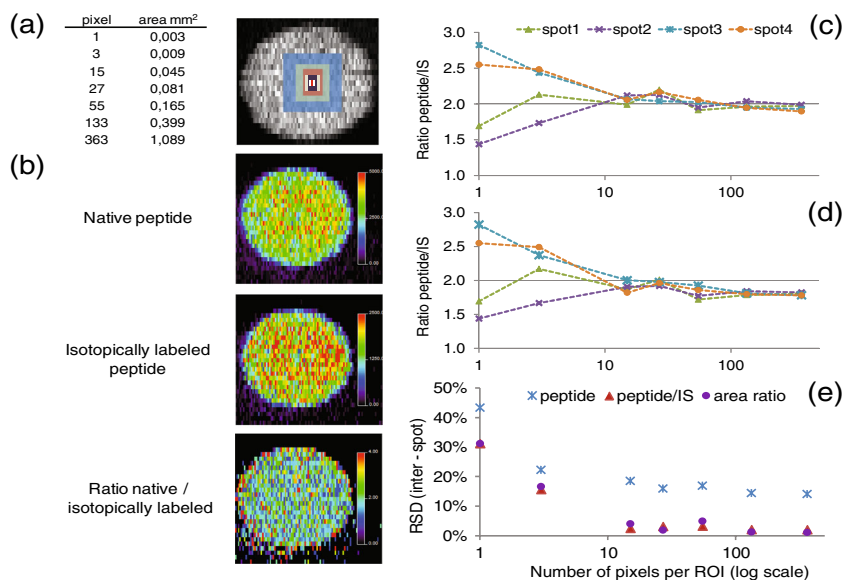
Besides the instrumental variability, the main challenge for absolute quantification remains the quest for the perfect dilution series to better mimic the behavior of an analyte in its biological environment. While MSI is a quantitative tool regarding the amount per surface, future efforts will have to be directed toward the generation of robust approaches to make MALDI-MSI a fully established tool for absolute quantification.

References

1. McDonnell LA, Piersma SR, Altelaar AFM, Mize TH, Luxembourg SL, Verhaert PDEM, Van Minnen J, Heeren RMA (2005) Subcellular imaging mass spectrometry of brain tissue. J Mass Spectrom 40(2):160–168. doi:10.1002/jms.735
2. Prideaux B, Stoeckli M (2012) Mass spectrometry imaging for drug distribution studies. J Proteomics 75(16):4999–5013. doi:10.1016/j.jprot.2012.07.028
3. Norris JL, Caprioli RM (2013) Analysis of tissue specimens by matrix-assisted laser desorption/ionization imaging mass spectrometry in biological and clinical research. Chem Rev 113(4):2309–2342. doi:10.1021/cr3004295
4. Minerva L, Ceulemans A, Baggerman G, Arckens L (2012) MALDI MS imaging as a tool for biomarker discovery: methodological challenges in a clinical setting. Proteomics Clin Appl 6:581–595. doi:10.1002/prca.201200033
5. Hamm G, Hochart G, Pamelard F, Legouffe R, Bonnel D, Stauber J (2013) Evaluation of quantitative MSI approaches applied to small and large molecules analysis in tissue. In: 61th ASMS Conference on Mass Spectrometry and Allied Topics, Salt Lake City, UT, June 9–13, 2013
6. Lietz CB, Gemperline E, Li L (2013) Qualitative and quantitative mass spectrometry imaging of drugs and metabolites. Adv Drug Delivery Rev. doi:10.1016/j.addr.2013.04.009
7. Solon EG, Schweitzer A, Stoeckli M, Prideaux B (2010) Autoradiography, MALDI-MS, and SIMS-MS imaging in pharmaceutical discovery and development. AAPS J 12(1):11–26. doi:10.1208/s12248-009-9158-4
8. Hattori K, Kajimura M, Hishiki T, Nakanishi T, Kubo A, Nagahata Y, Ohmura M, Yachie-Kinoshita A, Matsuura T, Morikawa T, Nakamura T, Setou M, Suematsu M (2010) Paradoxical ATP elevation in ischemic penumbra revealed by quantitative imaging mass spectrometry. Antioxid Redox Signal 13(8):1157–1167. doi:10.1089/ars.2010.3290
9. Signor L, Varesio E, Staack RF, Starke V, Richter WF, Hopfgartner G (2007) Analysis of erlotinib and its metabolites in rat tissue sections by MALDI quadrupole time-of-flight mass spectrometry. J Mass Spectrom 42(7):900–909. doi:10.1002/jms.1225
10. Takai N, Tanaka Y, Inazawa K, Saji H (2012) Quantitative analysis of pharmaceutical drug distribution in multiple organs by imaging mass spectrometry. Rapid Commun Mass Spectrom 26(13):1549–1556. doi:10.1002/Rcm.6256
11. Knochenmuss R, Dubois F, Dale MJ, Zenobi R (1996) The matrix suppression effect and ionization mechanisms in matrix-assisted laser desorption/ionization. Rapid Commun Mass Spectrom 10(8):871–877. doi:10.1002/(Sici)1097-0231(19960610)10:8<871::Aid-Rcm559>3.0.Co;2-R
12. Hamm G, Bonnel D, Legouffe R, Pamelard F, Delbos JM, Bouzom F, Stauber J (2012) Quantitative mass spectrometry imaging of propranolol and olanzapine using tissue extinction calculation as normalization factor. J Proteomics 75(16):4952–4961. doi:10.1016/j.jprot.2012.07.035
13. Nilsson A, Forngren B, Bjurstroem S, Goodwin RJA, Basmaci E, Gustafsson I, Annas A, Hellgren D, Svanhagen A, Andren PE, Lindberg J (2012) In situ mass spectrometry imaging and ex vivo characterization of renal crystalline deposits induced in multiple preclinical drug toxicology studies. PLoS ONE 7. doi:10.1371/journal.pone.0047353
14. Koeniger SL, Talaty N, Luo Y, Ready D, Voorbach M, Seifert T, Cepa S, Fagerland JA, Bouska J, Buck W, Johnson RW, Spanton S (2011) A quantitation method for mass spectrometry imaging. Rapid Commun Mass Spectrom 25:503–510. doi:10.1002/rcm.4891
15. Goodwin RJ, Mackay CL, Nilsson A, Harrison DJ, Farde L, Andren PE, Iverson SL (2011) Qualitative and quantitative MALDI imaging of the positron emission tomography ligands raclopride (a D2 dopamine antagonist) and SCH 23390 (a D1 dopamine antagonist) in rat brain tissue sections using a solvent-free dry matrix application method. Anal Chem 83(24):9694–9701. doi:10.1021/ac202630t
16. Hare DJ, Lear J, Bishop D, Beavis A, Doble PA (2013) Protocol for production of matrix-matched brain tissue standards for imaging by laser ablation-inductively coupled plasma-mass spectrometry. Anal Methods 5:1915–1921. doi:10.1039/C3AY26248K
17. Groseclose MR, Castellino S (2013) A mimetic tissue model for the quantification of drug distributions by MALDI imaging mass spectrometry. Anal Chem 85(21):10099–10106. doi:10.1021/ac400892z
18. Stoeckli M, Staab D, Schweitzer A (2007) Compound and metabolite distribution measured by MALDI mass spectrometric imaging in whole-body tissue sections. Int J Mass Spectrom 260:195–202. doi:10.1016/j.ijms.2006.10.007
19. Baluya DL, Garrett TJ, Yost RA (2007) Automated MALDI matrix deposition method with inkjet printing for imaging mass spectrometry. Anal Chem 79(17):6862–6867. doi:10.1021/ac070958d
20. Nilsson A, Fehniger TE, Gustavsson L, Andersson M, Kenne K, Marko-Varga G, Andren PE (2010) Fine mapping the spatial distribution and concentration of unlabeled drugs within tissue microcompartments using imaging mass spectrometry. PLoS ONE 5(7):e11411. doi:10.1371/journal.pone.0011411
21. Duncan MW, Roder H, Hunsucker SW (2008) Quantitative matrix-assisted laser desorption/ionization mass spectrometry. Brief Funct Genomics Proteomics 7(5):355–370. doi:10.1093/bfgp/eln041
22. Hilario M, Kalousis A, Pellegrini C, Müller M (2006) Processing and classification of protein mass spectra. Mass Spectrom Rev 25(3):409–449. doi:10.1002/mas.20072
23. Kaellback P, Shariatgorji M, Nilsson A, Andren PE (2012) Novel mass spectrometry imaging software assisting labeled normalization and quantitation of drugs and neuropeptides directly in tissue sections. J Proteomics 75:4941–4951. doi:10.1016/j.jprot.2012.07.034
24. Sleno L, Volmer DA (2005) Some fundamental and technical aspects of the quantitative analysis of pharmaceutical drugs by matrix-assisted laser desorption/ionization mass spectrometry. Rapid Comm Mass Spectrom 19(14):1928–1936. doi:10.1002/rcm.2006
25. Sleno L, Volmer DA (2006) Assessing the properties of internal standards for quantitative matrix-assisted laser desorption/ionization mass spectrometry of small molecules. Rapid Commun Mass Spectrom 20(10):1517–1524. doi:10.1002/rcm.2498
26. Reich RF, Cudzilo K, Levisky JA, Yost RA (2010) Quantitative MALDI-MSn analysis of cocaine in the autopsied brain of a human cocaine user employing a wide isolation window and internal standards. J Am Mass Spectrom 21(4):564–571. doi:10.1016/j.jasms.2009.12.014
27. Porta T, Grivet C, Kraemer T, Varesio E, Hopfgartner G (2011) Single hair cocaine consumption monitoring by mass spectrometric imaging. Anal Chem 83(11):4266–4272. doi:10.1021/ac200610c
28. Clemis EJ, Smith DS, Camenzind AG, Danell RM, Parker CE, Borchers CH (2012) Quantitation of spatially-localized proteins in

tissue samples using MALDI-MRM imaging. Anal Chem 84(8): 3514–3522. doi:10.1021/ac202875d

29. Prideaux B, Dartois V, Staab D, Weiner DM, Goh A, Via LE, Barry CE 3rd, Stoeckli M (2011) High-sensitivity MALDI-MRM-MS imaging of moxifloxacin distribution in tuberculosis-infected rabbit lungs and granulomatous lesions. Anal Chem 83(6):2112–2118. doi:10.1021/ac1029049

30. Rohner TC, Staab D, Stoeckli M (2005) MALDI mass spectrometric imaging of biological tissue sections. Mech Ageing Dev 126(1):177–185. doi:10.1016/j.mad.2004.09.032

31. Wiseman JM, Ifa DR, Zhu Y, Kissinger CB, Manicke NE, Kissinger PT, Cooks RG (2008) Desorption electrospray ionization mass spectrometry: imaging drugs and metabolites in tissues. Proc Natl Acad Sci 105(47):18120–18125. doi:10.1073/pnas.0801066105

32. Pirman DA, Kiss A, Heeren RM, Yost RA (2013) Identifying tissue-specific signal variation in MALDI mass spectrometric imaging by use of an internal standard. Anal Chem 85(2):1090–1096. doi:10.1021/ac3029618

33. Pirman DA, Yost RA (2011) Quantitative tandem mass spectrometric imaging of endogenous acetyl-L-carnitine from piglet brain tissue using an internal standard. Anal Chem 83(22):8575–8581. doi:10.1021/ac201949b

34. Pirman DA, Reich RF, Kiss A, Heeren RMA, Yost RA (2013) Quantitative MALDI tandem mass spectrometric imaging of cocaine from brain tissue with a deuterated internal standard. Anal Chem 85:1081–1089. doi:10.1021/ac302960j

35. Ellis SR, Bruinen AL, Heeren RM (2014) A critical evaluation of the current state-of-the-art in quantitative imaging mass spectrometry. Anal Bioanal Chem 406(5):1275–1289. doi:10.1007/s00216-013-7478-9

36. Kovarik P, Grivet C, Bourgogne E, Hopfgartner G (2007) Method development aspects for the quantitation of pharmaceutical compounds in human plasma with a matrix-assisted laser desorption/ionization source in the multiple reaction monitoring mode. Rapid Commun Mass Spectrom 21(6):911–919. doi:10.1002/rcm.2912

37. Wagner M, Varesio E, Hopfgartner G (2008) Ultra-fast quantitation of saquinavir in human plasma by matrix-assisted laser desorption/ionization and selected reaction monitoring mode detection. J Chromatogr B 872(1–2):68–76. doi:10.1016/j.jchromb.2008.07.009

38. Lesur A, Varesio E, Domon B, Hopfgartner G (2012) Peptides quantification by liquid chromatography with matrix-assisted laser desorption/ionization and selected reaction monitoring detection. J Proteome Res 11(10):4972–4982. doi:10.1021/pr300514u

39. Lesur A, Varesio E, Hopfgartner G (2010) Accelerated tryptic digestion for the analysis of biopharmaceutical monoclonal antibodies in plasma by liquid chromatography with tandem mass spectrometric detection. J Chromatogr A 1217(1):57–64. doi:10.1016/j.chroma.2009.11.011

40. Simmons DA (2008) Improved MALDI-MS imaging performance using continuous laser rastering. Technical note, Applied Biosystems/MDS Sciex

41. Spraggins JM, Caprioli RM (2011) High-speed MALDI-TOF imaging mass spectrometry: rapid ion image acquisition and considerations for next generation instrumentation. J Am Soc Mass Spectrom 22(6):1022–1031. doi:10.1007/s13361-011-0121-0

42. Claude E, Snel M, McKenna T, Langridge J (2008) Increasing the spatial resolution of MALDI images by oversampling. Application note, Waters

43. Snel MF, Fuller M (2010) High-spatial resolution matrix-assisted laser desorption ionization imaging analysis of glucosylceramide in spleen sections from a mouse model of Gaucher disease. Anal Chem 82:3664–3670. doi:10.1021/ac902939k

44. Dreisewerd K, Schürenberg M, Karas M, Hillenkamp F (1995) Influence of the laser intensity and spot size on the desorption of molecules and ions in matrix-assisted laser desorption/ionization with a uniform beam profile. Int J Mass Spectrom Ion Process 141(2):127–148. doi:10.1016/0168-1176(94)04108-J

45. Porta T, Grivet C, Knochenmuss R, Varesio E, Hopfgartner G (2011) Alternative CHCA-based matrices for the analysis of low molecular weight compounds by UV-MALDI-tandem mass spectrometry. J Mass Spectrom 46:144–152. doi:10.1002/jms.1875

46. Corr JJ, Kovarik P, Schneider BB, Hendrikse J, Loboda A, Covey TR (2006) Design considerations for high speed quantitative mass spectrometry with MALDI ionization. J Am Soc Mass Spectrom 17(8):1129–1141. doi:10.1016/j.jasms.2006.04.026

47. Hatsis P, Brombacher S, Corr JJ, Kovarik P, Volmer DA (2003) Quantitative analysis of small pharmaceutical drugs using a high repetition rate laser matrix-assisted laser/desorption ionization source. Rapid Commun Mass Spectrom 17(20):2303–2309. doi:10.1002/rcm.1192

48. Gobey J, Cole M, Janiszewski J, Covey T, Chau T, Kovarik P, Corr J (2005) Characterization and performance of MALDI on a triple quadrupole mass spectrometer for analysis and quantification of small molecules. Anal Chem 77(17):5643–5654. doi:10.1021/ac0506130

49. Norris JL, Cornett DS, Mobley JA, Andersson M, Seeley EH, Chaurand P, Caprioli RM (2007) Processing MALDI mass spectra to improve mass spectral direct tissue analysis. Int J Mass Spectrom 260(2–3):212–221. doi:10.1016/j.ijms.2006.10.005

50. Jaskolla TW, Karas M, Roth U, Steinert K, Menzel C, Reihs K (2009) Comparison between vacuum sublimed matrices and conventional dried droplet preparation in MALDI-TOF mass spectrometry. J Am Soc Mass Spectrom 20(6):1104–1114. doi:10.1016/j.jasms.2009.02.010

51. Murphy RC, Hankin JA, Barkley RM, Zemski Berry KA (2011) MALDI imaging of lipids after matrix sublimation/deposition. Biochim et Biophys Acta (BBA) - Mol Cell Biol Lipids 1811(11):970–975. doi:10.1016/j.bbalip.2011.04.012